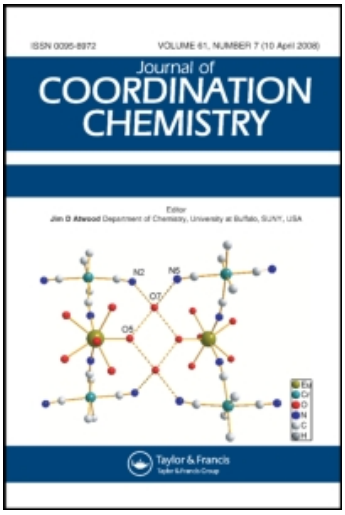

Journal of Coordination Chemistry
Publication details, including instructions for authors and subscription information:
http://www.informaworld.com/smpp/title~content=t713455674

AQUEOUS EQUILIBRIA OF COPPER(II)- AND NICKEL(II)-POLYGLYCINE COMPLEXES

A. Kaneda[a]; A. E. Martell[a]
[a] Chemistry Department, Texas A & M University, College Station, Texas, U.S.A.

To cite this Article Kaneda, A. and Martell, A. E.(1975) 'AQUEOUS EQUILIBRIA OF COPPER(II)- AND NICKEL(II)-POLYGLYCINE COMPLEXES', Journal of Coordination Chemistry, 4: 3, 137 — 151
To link to this Article: DOI: 10.1080/00958977508075892
URL: http://dx.doi.org/10.1080/00958977508075892

J. Coord. Chem.
1975, Vol. 4, pp. 137–151

AQUEOUS EQUILIBRIA OF COPPER(II)- AND NICKEL(II)-POLYGLYCINE COMPLEXES

A. KANEDA and A. E. MARTELL†

Chemistry Department, Texas A & M University, College Station, Texas 77843, U.S.A.

(Received November 8, 1974)

Magnetic susceptibility measurements, new potentiometric data, optical spectra, and a new statistical method of calculation are combined in the formulation of an equilibrium scheme defining the dilute solution interactions of nickel(II) and copper(II) ions with diglycine, triglycine, and tetraglycine as a function of pH. At low pH appreciable concentrations of a previously unreported complex, MHL^{2+} (HL = polyglycine ligands) are shown to be present in all nickel(II)-polyglycine systems and in the copper(II)-triglycine system. This new protonated species is assigned a structure in which the metal ion is coordinated to the terminal carboxylate and to the adjacent peptide carbonyl oxygen with the proton residing on the terminal amino group. As the pH is raised in the 1:1 systems, $MH_{-1}L$, $MH_{-2}L^{-}$ and $MH_{-3}L^{2-}$ are formed in succession depending on the number of peptide linkages in the ligands, HL. The concentration of the monodeprotonated intermediate species $NiH_{-1}L$ never exceeds 10% of the total metal ion concentration in the triglycine case and is always less than 0.5% when tetraglycine is the ligand. The dideprotonated intermediate $NiH_{-2}L^{-}$ reaches a maximum of 38% of the total metal concentration in the 1:1 Ni-tetraglycine system. An explanation is presented for this negative deviation from the predictions based on statistical grounds. Complete species distribution diagrams which include the new protonated complexes are presented and are employed to explain the differences in the interactions of copper(II) and nickel(II) ions with polyglycine ligands. Probable coordinate bonding sites suggested for the complexes formed in solution are inferred on the basis of stoichiometry, relative stabilities, and available microscopic information.

INTRODUCTION

The aqueous equilibria of the copper(II) and nickel(II)-complexes has been the subject of many investigations, and the interpretations offered have varied in some respects. For example, direct evidence for the copper(II) and nickel(II)-promoted deprotonation reactions of peptide linkages was obtained from aqueous infrared spectra of the complexes formed in solution[1–5] and from X-ray crystallographic studies[6] for copper(II)-polypeptides in the solid state. From a detailed review of previous work, and related infrared spectral assignments reported by Martell,[7] and by Martell and Kim,[8] it became apparent that there are several unsolved problems that require further study, such as the inadequacy of low pH equilibrium data for the nickel(II) and copper(II)-polyglycine systems, and the details of the deprotonation process in Ni(II)-tri- and tetraglycine systems.

A potentiometric study by Osterberg[9] over a wide range of concentration of Cu(II) and triglycine revealed the presence of a protonated complex species at low pH as well as the formation of polynuclear species in solutions of high concentration. Kim and Martell[5,10] studied the proton nmr spectra of copper(II) and nickel(II) polyglycines and suggested the presence of a species involving the coordination of the metal ion through the carboxylate group in Ni(II)-polyglycine systems at low pH. A detailed characterization of the protonated species has not been made and other workers overlooked the presence of such species in their studies.

Kim and Martell[3] suggested that the peptide protons of Ni(II)-triglycine and tetraglycine seem to be displaced simultaneously, in contrast to the stepwise dissociation proposed by Martin *et al.*[11]

A comparison of the reported equilibrium constants governing the copper(II)- and nickel(II) interactions shows that the values published by various workers[12–16] differ markedly in magnitude. These inconsistencies in the reported metal-polyglycine equilibria may arise partially from differences in the mathematical treatment of the potentiometric data,[17] but may also be due to differences in conventions, electrode calibration, and solution conditions.

The purpose of this paper is to establish a consistent, rigorous equilibrium scheme for copper(II)- and nickel(II)-polyglycine complexes in dilute solution, to characterize all the major species

†This work was supported by a research grant A-259 from the Robert A. Welch Foundation.

formed, and to propose reasonable structures for these species. In addition to the use of a newly-developed statistical mathematical treatment to obtain a consistent set of formation constants, new magnetic susceptibility measurements and optical spectra will be employed for elucidation of the complexes formed.

EXPERIMENTAL

Reagents

Diglycine, triglycine and tetraglycine (K & K Laboratories), after recrystallization twice from water/ethanol, were found to be 99.8–99.9% pure as determined by potentiometric titration with standard base.[18] Solutions of copper(II) nitrate and nickel(II) nitrate were standardized by titration with standard EDTA solution. 2-Pyridyl methyl ketone (Eastman), was the highest grade available (analytical grade) and was used without further purification.

Potentiometric Titrations

The potentiometric measurements of ligand-base and metal-ligand equilibria were carried out under nitrogen at 25.0° at an ionic strength of 0.10 M, adjusted with potassium nitrate. A Beckman Research Model 101900 pH meter, fitted with Beckmann 39000 glass and 39071 calomel electrodes, was employed. Before each experiment, the pH meter-electrode system was calibrated in terms of hydrogen ion concentration by the titration of 0.0100 M hydrochloric acid with 0.100 M CO_2-free potassium hydroxide solution. The concentration ion product constant under the conditions employed was determined from the data compiled by Harned and Owen[19] to be $10^{-13.792}$

Magnetic Susceptibility Measurements

The magnetic susceptibility measurements of the Ni(II)-triglycine and tetraglycine solutions were made with a Varian Model A-60 nmr spectrometer by the method described by Evans.[20] Samples containing 0.020 M of the 1:1 Ni(II)-polyglycine complex and 2% t-butanol were prepared by adding base from $m = 0$ to $m = 3$ and from $m = 0$ to $m = 4$ for the Ni(II)-tri- and tetraglycine complex systems, respectively (m = moles of base added per mole of metal ion). An inner tube containing 2% t-butanol solution was placed in each sample tube as a reference. The method was calibrated by measuring the frequency shifts of 0.0200 M nickel(II) chloride solutions under the same conditions.

Electronic Spectra Measurements

The Copper(II)-triglycine System The electronic spectra of copper(II)-triglycine system was measured as a function of the base added at ambient room temperature ($25 \pm 3°$) with constant ligand concentration of 0.010 M and constant ionic strength of 0.10 M in potassium chloride. The measurements were made with a Cary 14 spectrophotometer, using 1.000 cm matched quartz cells.

The Nickel(II)-Schiff Base Complex System The electronic spectra of the 1:1:1 nickel(II):2-pyridylmethylketone:glycyl-DL-alanine system was measured as a function of the base added. All measurements were made with a constant ligand concentration of 1.000×10^{-3} M. After measurement, the $-\log [H^+]$ of every sample was determined with a Beckman Research model 101900 pH meter, fitted with a Sargent 30070-10 glass-calomel combination electrode.

Calculations

Overlapping equilibrium constants were calculated with a new statistical approach designed to eliminate the necessity of accurate imput guesses in order to achieve further refinement of the data. The "pit mapping" program LETAGROP requires approximate constants within ±0.1 log units as initial guesses in order for convergence to occur.

By combining mass balance and proton balance equations, a given equilibrium constant may be expressed as a function of one or more other constants involved in the same equilibrium system. For two overlapping constants, the relationship may be represented by Eq. (1).

$$K_1 = f(K_2) \tag{1}$$

It is conventional to plot K_1 as a function of K_2 for all experimental data points and to evaluate the constants from the intercepts of the lines thus produced.[21] In the present work, this treatment was extended further to the cases of three and four overlapping constants by defining an error function Y as a function of the other equilibrium constants as indicated by Eq. (2):

$$Y = \Sigma(\sigma_{K_1})^2 = f(K_2, K_3 \ldots K_r) \tag{2}$$

The error function is defined as the sum of the squares of the deviation in the calculated constant over the calculation range. When this error function is minimized the corresponding values of $K_1, K_2 \ldots K_r$

should be the "best" equilibrium constants for the system.

While a modification of the pit-mapping technique[22,23] was employed to find the minimum, the present method has the following advantages: 1, the quadratic equation is reduced by one dimension, and 2, the shapes of the error distribution around the minimum become more symmetric than is the case for previous techniques[9,22,23] (in which the error function is defined as the sum of the squares of deviations in the calculated "a" values, T_M or $-\log[H^+]$. Also, in the present treatment, the general graphical method that would otherwise be employed to obtain the approximate initial values for the least square refinements has been eliminated.

The FORTRAN IV computer program employed was designed to calculate up to four overlapping equilibrium constants. The relationship between the constants, Eq. (2), is set in a subroutine program and the main program remains unchanged for each type of calculation. For example, in the case of three overlapping constants, the shape of the error distribution around the minimum may be approximated by a quadratic equation:

$$Y = a_1K_2^2 + a_2K_3^2 + a_3K_3K_2 + a_4K_2 + a_5K_3 + a_6 \quad (3)$$

The coefficients $a_1 - a_6$ are determined from a set of six simultaneous equations of the type of equation (3) at $K_2' \pm \Delta$ and $K_3' \pm \Delta$, where K_2' and K_3' are the initial guesses and Δ is an appropriate increment. By taking the partial derivatives of Y with respect to K_2 and K_3, and by solving the simultaneous equation thus produced, the minimum value of Y in Eq. (3) may be obtained. The improved values of K_2 and K_3 at the minimum are then reprocessed through Eqs. (1) and (3) and the procedure is repeated until the best values of K_1, K_2 and K_3 are obtained.

Then the "a" values (mole of base added per mole of ligand) corresponding to the experimental $-\log[H^+]$ values are calculated with a subroutine program. In the course of the calculation free ligand concentrations are obtained by means of the Newton-Raphson method. Each final set of constants is then verified by checking whether the calculated K_1 values remain constant over wide pH ranges and whether the calculated "a" values coincide with the experimental "a" values. The approximate initial values needed in the calculation are obtained by using the treatment for two overlapping constants in a relatively restricted pH range. Then, three (or four) overlapping constants are calculated over the whole buffer region. All calculations were made with the aid of an IBM 360-65 computer at the Data Processing Center of Texas A & M University. The computer program was written in FORTRAN IV, and details of the calculations and program employed have been described by Kaneda.[24]

RESULTS

New Stability Data

Before any further calculations could be carried out, reliable sets of protonation constants were needed and were determined from the potentiometric equilibrium measurements in the absence of metal ions. These new values measured at 25.0 ± 0.1° in 0.100 M KNO_3 are listed in Table I.

TABLE I
Proton association constants of oligoglycines at 25° (0.100 M KNO_3)

Ligand	Log K_1^H ($-NH_2$)[a]	Log K_2^H ($-COOH$)[a]
diglycine (gg)	8.07	3.18
triglycine (ggg)	7.88	3.25
tetraglycine (gggg)	7.79	3.28

[a] All values reliable to ± 0.01 log units.

The relationships which were necessary to describe the equilibria of the metal complex species formed under varied conditions of stoichiometry, concentration and pH, and the symbols for the corresponding equilibrium quotients, are listed as Eqs. 4–15. The symbol "n" is the number of peptide linkages present in the polypeptide being considered. The values of the equilibrium constants obtained with the newly developed procedure described above are presented in Table II.

$$M^{2+} + HL^{\pm} \rightleftharpoons MHL^{2+} \qquad K_{MHL} \quad (4)$$

$$MHL^{2+} \rightleftharpoons ML^{+} + H^{+} \qquad K_{ML}^{H} \quad (5)$$

$$M^{2+} + L^{-} \rightleftharpoons ML^{+} \qquad K_1 \quad (6)$$

$$ML^{+} + L^{-} \rightleftharpoons ML_2 \qquad K_2 \quad (7)$$

$$ML^{+} \rightleftharpoons MH_{-1}L + H^{+} \qquad K_{1a} \quad (8)$$

$$MH_{-1}L \rightleftharpoons MH_{-2}L^{-} + H^{+} \qquad K_{1b} \quad (9)$$

TABLE II
Equilibrium constants of oligoglycine complexes of copper(II) and nickel(II) at 25.0 ± 0.1° (0.10 M KNO_3)

Equilibrium Constants	Diglycine		Triglycine		Tetraglycine	
	Cu^{2+}	Ni^{2+}	Cu^{2+}	Ni^{2+}	Cu^{2+}	Ni^{2+}
Log K_{MHL}	0.07[a]	2.69[g]	2.36[d]	2.86[i]	0.80[e]	3.12[o]
pK^{H}_{ML}	2.47[a]	6.29[g]	5.02[c,d]	6.58[i]	3.53[e]	6.60[o]
Log K_1	5.68[a]	3.88[f]	5.08[c]	3.72[h,i,k]	5.16[e]	3.63[l]
Log K_2		3.12[f]		2.79[h]		2.78[l]
pK_{1a}	4.21[a]	8.88[g]	5.16[c,d]	8.91[h,i,k]	5.52[e]	
pK_{1b}			6.74[c]	7.83[k]	6.78[e]	
pK_{1c}					9.16	8.1[m]
pK_{1ab}				16.74[j]		15.8[l,m,o]
pK_{1abc}						24.22[n]
pK_{h1}	9.24[b]		11.5			
Log K_d	2.15[b]					
Log K'_2	2.84[b]					

Average deviations of the calculated "a" values compared to the experimental curve [a]±0.003; [b]±0.008; [c]±0.003; [d]±0.002; [e]±0.005; [f]±0.006; [g]±0.001; [h]±0.005; [i]±0.001; [j]±0.01; [k]±0.005; [l]±0.006; [m]±0.01; [n]±0.02; [o]±0.006.

$$MH_{-2}L^{-} \rightleftharpoons MH_{-3}L^{2-} + H^{+} \qquad K_{1c} \qquad (10)$$

$$ML^{+} \rightleftharpoons MH_{-2}L^{-} + 2H^{+} \qquad K_{1ab} \qquad (11)$$

$$ML^{+} \rightleftharpoons MH_{-3}L^{2-} + 3H^{+} \qquad K_{1abc} \qquad (12)$$

$$MH_{-n}L^{(n-1)-} \rightleftharpoons MH_{-n}L(OH)^{n-} + H^{+} \qquad K_{h1} \qquad (13)$$

$$MH_{-1}L(OH)^{-} + MH_{-1}L \rightleftharpoons (MH_{-1}L)_2OH^{-} \qquad K_d \qquad (14)$$

$$MH_{-1}L + L^{-} \rightleftharpoons M(H_{-1}L)L^{-} \qquad K'_2 \qquad (15)$$

The concentrations of the complex species determined by methods described above, and calculated with the equilibrium constants presented in Table II are presented as plots of degree of formation *vs.* $-\log[H^+]$ in Figures 1–4 for the copper(II) complexes, and in Figures 5–8 for the nickel(II) complexes. These distribution curves have the advantage of representing visually the rise and fall of concentration of each species as the pH is increased through the range employed in this investigation.

The species distribution diagram shown in Figure 3 indicates the presence of $CuHL^{2+}$ when triglycine is the ligand. Likewise, Figures 5–8 indicate the presence of $NiHL^{2+}$ for the diglycine, triglycine, and

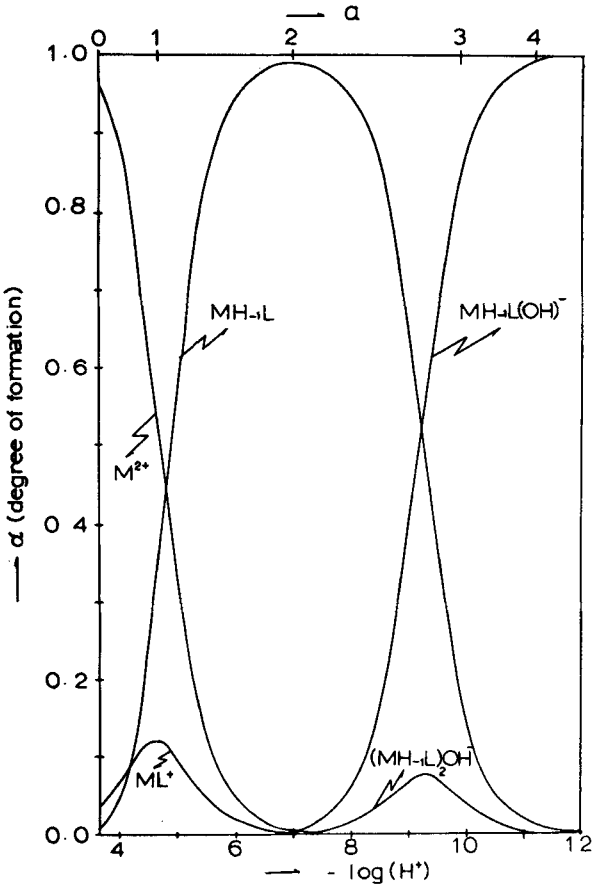

FIGURE 1 Ionic species distribution diagram for 1:1 (Cu(II)-digylcine systems; Degree of formation of each ionic species vs. $-\log [H^+]$ and "a" value; $T_M = T_L = 2.073 \times 10^{-3}$ M, at 25°, $\mu = 0.10$ (KNO_3); concentration of $CuHL^{2+}$ can be neglected, less than $\alpha = 0.01$.

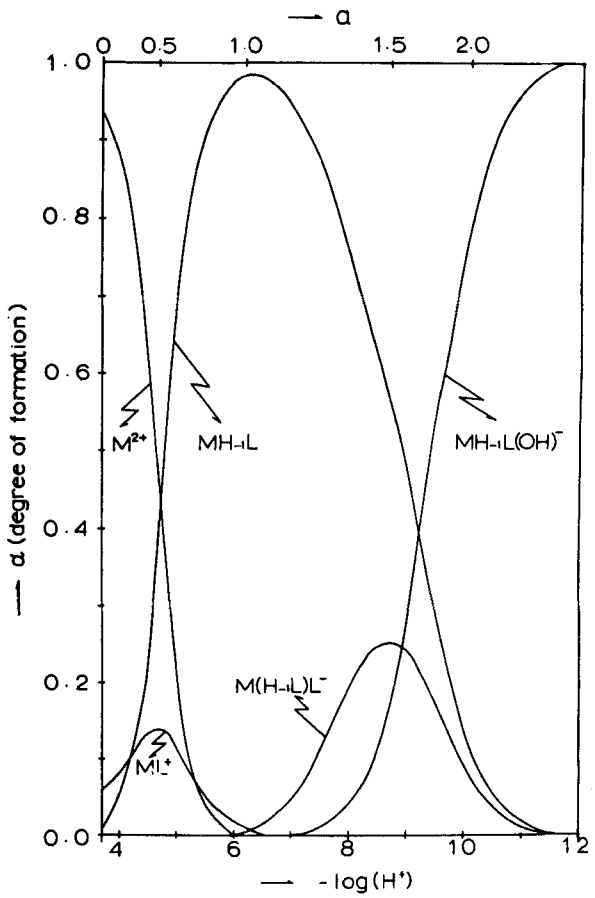

FIGURE 2 Ionic species distribution diagram for 1:2 Cu(II)-diglycine system; $T_L = 2.073 \times 10^{-3}$ M, $T_M = 1.036 \times 10^{-3}$ M, at 25°, $\mu = 0.10$ (KNO_3).

tetraglycine systems. These protonated chelates are new since previous workers have not suggested their presence.

The electronic spectra of the Cu(II)-triglycine system as a function of pH are indicated in Figure 9. Figure 10 is a plot of both the experimental and the calculated molar susceptibilities against "m" (moles of base per mole of metal complex) for the nickel(II)-triglycine system. A similar plot for the nickel(II)-tetraglycine system is presented in Figure 11.

The electronic spectrum of the complex formed by a 1:1:1 ratio of nickel(II):2-pyridylmethyl-ketone:glycyl-DL-alanine had two absorption peaks at 380 nm and 410 nm (shoulder). The optical densities at 380 nm varies from 0 to 1.2 as the conditions are changed from a = 1 to $a = 2$, (a = moles of base added per mole of ligand), with its highest value at $a = 2$. Since excess of 2-pyridylmethylketone improved the optical density at $a = 2$ up to a 1:3 molar ratio ligand to ketone, the molar absorptivity of the yellow deprotonated Schiff base complex was calculated to be 3.19×10^3 at $\lambda_{max} = 380$ nm. The proton dissociation constant for conversion of the chelate NiL^+ to $NiH_{-1}L$ was then calculated from the optical densities at 380 nm and $-\log[H^+]$ values of various samples: $-\log K_{1a} = 7.24 \pm 0.03$. The molar absorptivity of NiL^+ was estimated to be negligible under these conditions.

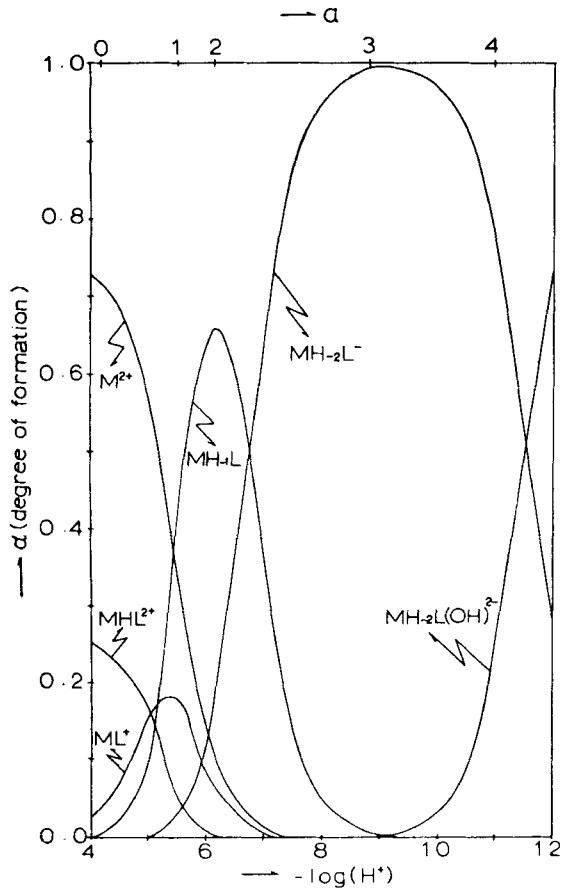

FIGURE 3 Ionic species distribution diagram for 1:1 Cu(II)-triglycine system; $T_M = T_L = 2.042 \times 10^{-3}$ M, at 25°, $\mu = 0.10$ (KNO_3); Since there is no formation of CuL_2, 1:2 system gives the same distribution diagram.

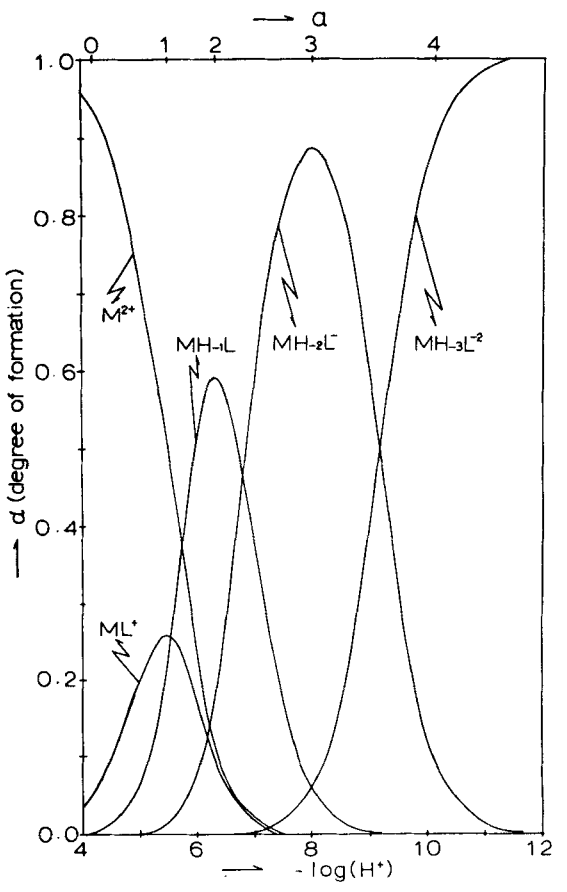

FIGURE 4 Ionic species distribution diagram for 1:1 Cu(II)-tetraglycine system; $T_M = T_L = 1.885 \times 10^{-3}$ M, at 25°, $\mu = 0.10$ (KNO_3); concentration of $CuHL^{2+}$ can be neglected, less than $\alpha = 0.012$.

DISCUSSION

The Protonated Species MHL^{2+}

The presence of the protonated species $CuHL^{2+}$ may be neglected in the cases of copper(II)-di-, and tetraglycine systems on the basis of the small values of log K_{MHL} as seen in Table II. The actual concentration of the species $CuHL^{2+}$ in these two systems was found to be less than 1% of the total metal ion concentration. However, an appreciable concentration of $CuHL^{2+}$ was detected in the copper(II)-triglycine system as illustrated in Figure. 3. While the calculated titration curves produced by either ignoring or considering $CuHL^{2+}$ in the treatment were very similar, a better fit was obtained through the incorporation of the protonated species.

The structures of the protonated species in acidic solution was inferred from electronic spectra. There appears to be no difference in the spectra measured at $m = -1.0$ and $m = -0.5$ where $[MHL^{2+}]$ is about 10% and $[M^{2+}]$ is about 90% of the metal species present. However, in the region where $[ML^+]$ begins to make a substantial contribution, the curve at $m = 0$ (C in Figure 9) is higher than A or B, indicating that ML^+ possesses a larger extinction coefficient than MHL^{2+}. If the $CuHL^{2+}$ had the structure proposed by Osterberg,[9] in which the copper(II) ion is coordinated to the terminal amino nitrogen and the adjacent peptide carbonyl oxygen and the additional

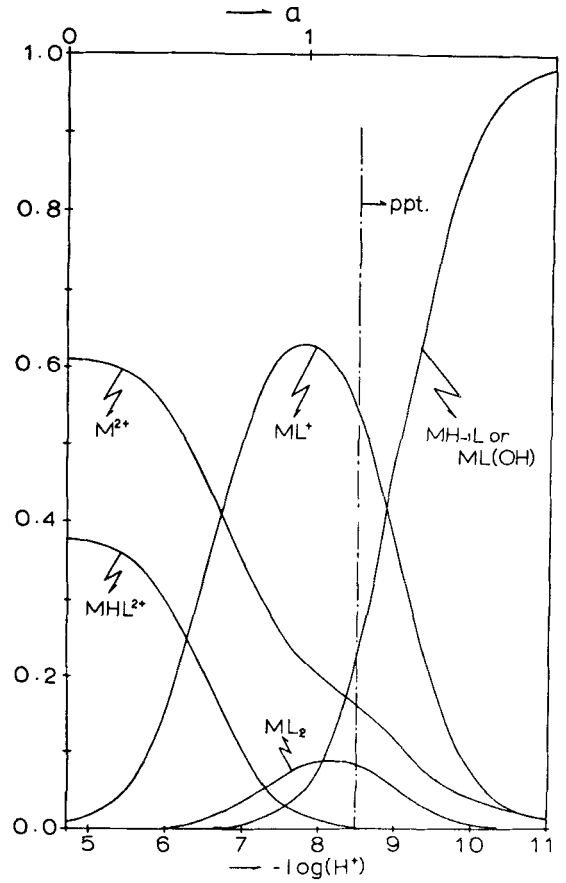

FIGURE 5 Ionic species distribution diagram for 1:1 Ni(II)-diglycine system; $T_M = T_L = 2.064 \times 10^{-3}$ M, at 25°, $\mu = 0.10$ (KNO_3); above $-\log [H^+] = 8.5$, precipitate was formed.

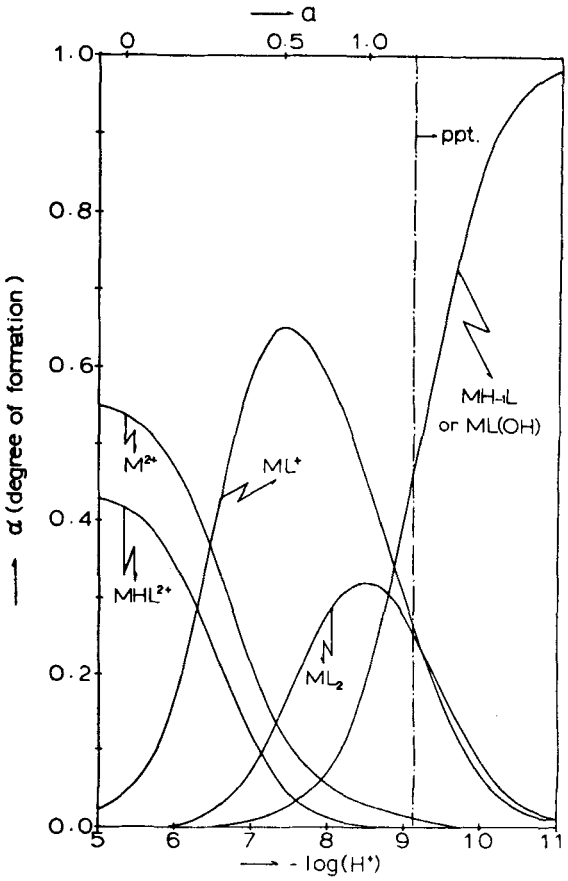

FIGURE 6 Ionic species distribution diagram for 1:2 Ni(II)-diglycine system; $T_M = 1.032 \times 10^{-3}$ M, $T_L = 2.064 \times 10^{-3}$ M, at 25°, $\mu = 0.10$ (KNO_3); above $-\log[H^+] = 9.1$, a precipitate was formed.

proton remains attached to the terminal carboxylate, then the extinction coefficient of $CuHL^{2+}$ would be expected to be very close to that of CuL^{+5}. If the extinction coefficients of $CuHL^{2+}$ and CuL^+ were very similar, this enhancement in electronic spectra peak should have been observed from $m = -1.0$ to $m = -0.5$. Therefore, based on the conclusions drawn from the spectra alone, the structure proposed by Osterberg may be eliminated.

Secondly, the value of $-\log K_{ML}{}^H = 6.58$ for Cu(II)-triglycine is higher than the first proton dissociation constant of the free ligand, $-\log K_2{}^H = 3.25$. If the additional proton of $CuHL^{2+}$ remains attached to the terminal carboxylates, then $-\log K_{ha}$ should be at least several orders of magnitude smaller than $-\log K_1{}^H$ because of $-I$ effects exerted by the central Cu(II) ion. The opposite is observed; i.e., $-\log K_{ML}{}^H > -\log K_1{}^H$, therefore consistent with both electronic spectra and pK_a considerations, the only other plausible structure would be the coordinated complex illustrated in Formula I.

However, based on the titration data the concentration of the protonated species $NiHL^{2+}$ in nickel(II)-di-, tri- and tetraglycine solutions is seen to be significant (see Figures 5, 7 and 8). Through inclusion of $NiHL^{2+}$ in the calculation, the average deviation of the calculated "a" value from the experimental value, DEV, was reduced substantially in each case. Further evidence for the presence and

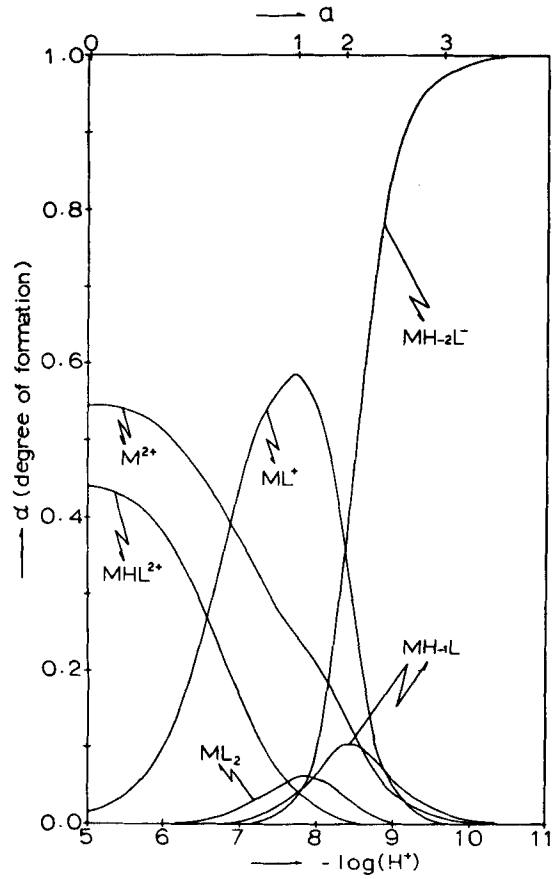

FIGURE 7 Ionic species distribution diagram for 1:1 Ni(II)-triglycine system; $T_M = T_L = 2.048 \times 10^{-3}$ M, at 25°, $\mu = 0.10$ (KNO_3).

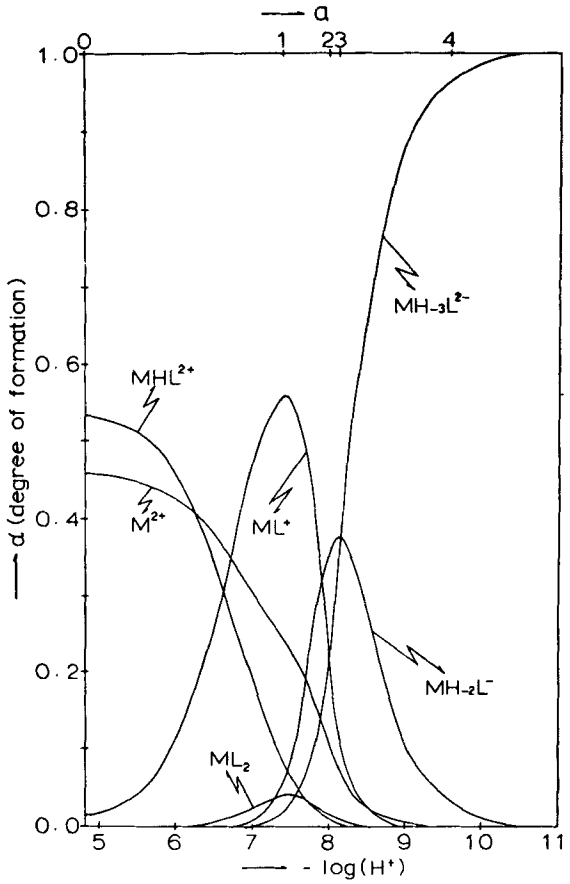

FIGURE 8 Ionic species distribution diagram for 1:1 Ni(II)-tetraglycine system; $T_M = T_L = 1.927 \times 10^{-3}$ M, at 25°, $\mu = 0.10$ (KNO_3).

structure of $NiHL^{2+}$ is provided in published IR data. The IR band at 1632 cm^{-1}, in the case of the nickel(II)-diglycine system for example, which is assigned to the asymmetric stretching frequency of the metal coordinated peptide carbonyl, was observed at $m = 0$ (pD = 5.05) where NiL^+ is not yet formed. However, the proportion of the protonated species $NiHL^{2+}$ comprises 37% of the total $[M^{2+}]$ concentration at $m = 0$. Therefore, if it is assumed that the metal ion is coordinated through the terminal carboxylate and the adjacent peptide carbonyl oxygen and that the additional proton remains on the terminal amino group, the IR band at 1632 cm^{-1} is readily explained.

In addition, the value $-\log K_{ML}{}^{H} = 6.20$ is much higher than the first dissociation constant of the ligand $-\log K_2{}^{H}$ (3.18) and less than $-\log K_1{}^{H}$ (8.07) the nickel(II)-diglycine system. The additional proton is attached to the terminal amino group, which experiences coulombic repulsions from the dipositive metal ion to make $-\log K_{ML}{}^{H}$ smaller than $-\log K_1{}^{H}$. This adds further support to the postulated structure of $NiHL^{1+}$. The following reactions are then reasonable on the basis of electrostatic considerations, infrared spectra, and calculated stability constants.

The same argument for the presence of and the structure of $NiHL.^{2+}$ can be made for the Ni(II)-tri- and tetraglycine systems.

The values of $\log K_{MHL}$ increase in the order di- < tri- < tetraglycine, as seen from the relative degrees of formation $NiHL^{2+}$ as shown in Figures 5, 7

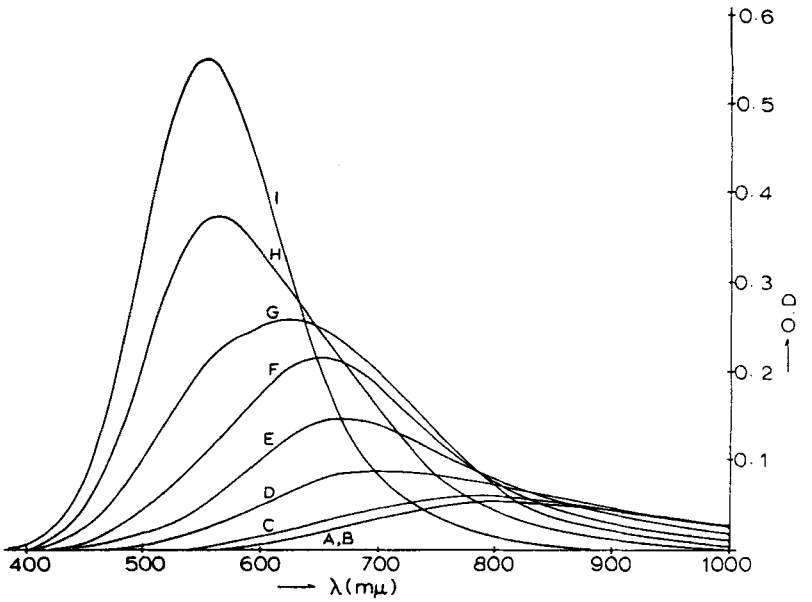

FIGURE 9 Electronic spectra of 1:1 Cu(II)-triglycine system; $T_M = T_L = 4.020 \times 10^{-3}$ M, at 25°, $\mu = 0.10$ (KNO_3); A, B, C, D, E, F, G, H and I correspond to the spectra at $m = -1.0, -0.5, 0.0, 0.5, 1.0, 1.5, 2.0, 2.5$ and 3.0, respectively.

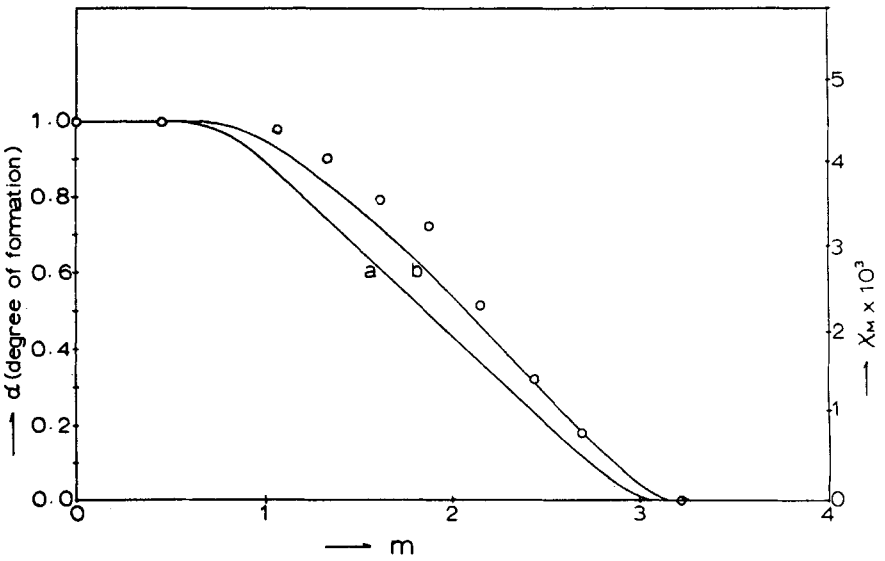

FIGURE 10 Magnetic susceptibilities of 1:1 Ni(II)-triglycine system; molar susceptibility vs. "m" value; circle points, experimental molar susceptibility; Curve a, the sum of degree of formation of paramagnetic species calculated from $pK_{1ab} = 16.74$; Curve b, the sum of degree of formation of paramagnetic species calculated from $pK_{1a} = 8.91$ and $pK_{1b} = 7.83$.

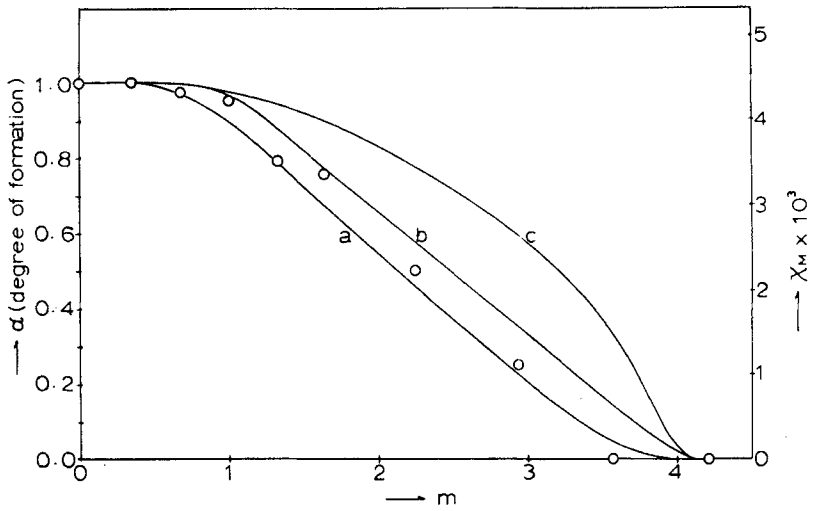

FIGURE 11 Magnetic susceptibilities of 1:1 Ni(II)-tetraglycine system; molar susceptibility vs. "m" value; circle points, experimental molar susceptibility; Curve a, the sum of degree of formation of paramagnetic species calculated from $pK_{1ab} = 15.8$ and $pK_{1c} = 8.1$; Curve b, the sum of degree of formation of paramagnetic species calculated from $pK_{1abc} = 24.22$; Curve c, the sum of degree of formation of paramagnetic species calculated from $pK_{1ab} = 15.8$ and $pK_{1c} = 8.1$ while $NiH_{-2}L^{-}$ was assumed to be paramagnetic; see discussion.

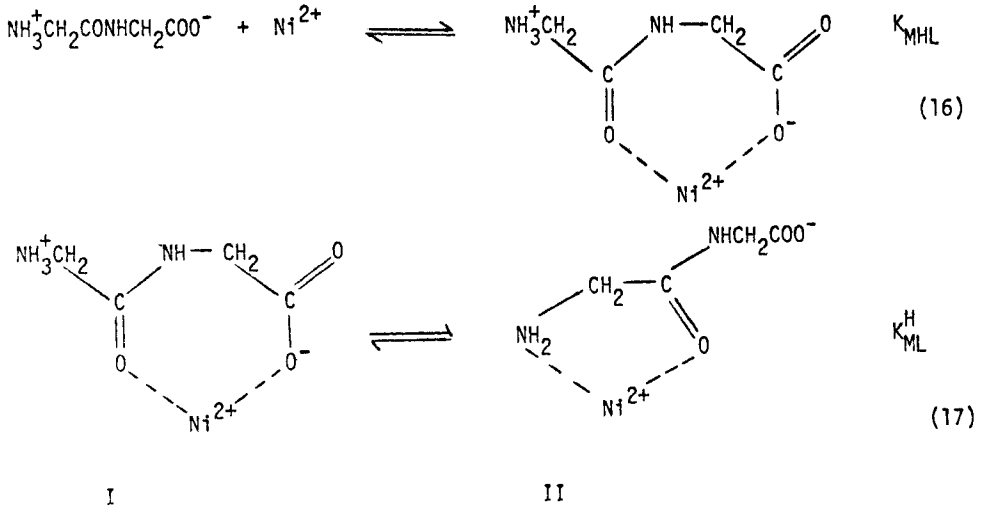

and 8. The values of $-\log K_{ML}{}^{H}$ also increase in the same order. This behavior is consistent with the decrease in the repulsive force between the positive metal ion and the protonated amino group, as the number of peptide linkages increases and the distance between the protonated terminal amino group and the central metal ion increases.

The deprotonation sequence of the protonated terminal amino group $-\log K_{ML}{}^{H}$ of glycylglycine is accompanied by coordination rearrangement from the terminal carboxylate to the terminal amino nitrogen to form a more stable NiL^{+} species with a five-membered ring, as shown in Eq. 17. Copper(II), on the other hand, possesses a stronger affinity

toward the amino nitrogen than does nickel(II), so that the low concentration of $CuHL^{2+}$ is reasonable and not entirely unexpected. In fact, the affinity of the copper(II) ion for amino nitrogen is so strong that the protonated terminal amino group may ionize before the metal ion can coordinate to the carboxylate oxygen to form the much less stable protonated species with a 7 membered ring. Thus the copper(II) reaction probably occurs directly as indicated in Eq. 18.

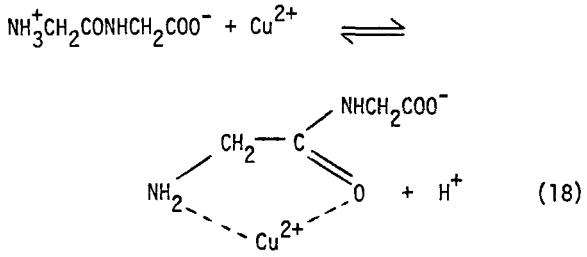

(18)

III

Further insight into the proposed structures of the protonated species may be gleaned from the proton nmr spectra of nickel(II)-di-, tri- and tetraglycine[5,10]. It had been shown that in neutral solution with increasing concentration of paramagnetic nickel(II) ion, the peak corresponding to the methylene group adjacent to the terminal carboxylate is the first to disappear in all nickel(II)-polyglycine systems. On the other hand, in the case of the copper(II)-polyglycines, both in neutral and in basic solution, the peak corresponding to the methylene group adjacent to the terminal amine is always the first to disappear. In the case of the nickel(II) polyglcines in basic solution, the terminal amino methylene was also the first to disappear. These observations support the above conclusions that nickel(II)-polyglycine complexes in neutral solution involve the coordination of the metal ion through the terminal carboxylate while Cu(II)-polyglycine complexes in both neutral and basic solutions and Ni(II)-polyglycine complexes in basic solution involve coordination through the terminal amino group.

Amide Deprotonation Schemes for Nickel(II)-tri- and tetraglycine Systems

Nickel(II)-Triglycine

Calculations indicate that in the Ni(II)-triglycine system the intermediate $NiH_{-1}L$ amounts to 10% of the total metal concentration at $m = 2$, as is shown in the species distribution diagram, Figure 7. Further support for this observation may be gleaned from magnetic susceptibility as a function of "m" values depicted in Figure 10. Curve A was calculated by assuming that $NiH_{-1}L$ is absent and that $NiH_{-2}L^{-}$ is diamagnetic. The sum of the degrees of formation of paramagnetic species, $\alpha_{M^{2+}} + \alpha_{MHL^{2+}} + \alpha_{ML^{+}} + \alpha_{ML_2}$, was calculated using $-\log K_{1ab} = 16.74$. Curve B was calculated from the sum $\alpha_{M^{2+}} + \alpha_{MHL^{2+}} + \alpha_{ML^{+}} + \alpha_{ML_2} + \alpha_{ML_{-1}L}$ using the results of the potentiometric study: $-\log K_{1a} = 8.91$ and $-\log K_{1b} = 7.83$. The open circles represent the experimental results, in which there was a trace of $Ni(OH)_2$ precipitate, but only in the region from $m = 1$, to $m = 2$. It is evident that Curve A differs markedly from the experimental curve throughout the whole region of $m = 1$ to $m = 3$, and that curve B gives a good fit to the experimental points in the region of $m = 2$ to $m = 3$, where the precipitate is absent. The slight deviation of Curve B in the region from $m = 1$ to $m = 2$ can be compensated for by estimating the amount of $Ni(OH)_2$ present.

The present results indicate that the amount of $NiH_{-1}L$ is much less than the 30% at $m = 2$ reported by Martin,[11] in agreement with data reported by Billo and Margerum.[25]

The curious observation that $-\log K_{1b}$ is smaller than $-\log K_{1a}$ may be readily explained on the basis of the structural change of the chelate from the octahedral (high spin) to the square planar (low spin) form as the second proton is dissociated. Since the best fit of the experimental molar susceptibility (Curve B), was produced by assuming that M^{2+}, MHL^{2+}, ML^{+}, ML_2 and $MH_{-1}L$ are paramagnetic while $MH_{-2}L^{-}$ is diamagnetic, the molar susceptibility measurements as a function of "m" provide direct evidence for this structural change.

Since the e_g orbitals are occupied by two unpaired electrons in $NiH_{-1}L$ (approximately octahedral) and the e_g orbitals are essentially antibonding orbitals, the electronic configuration change from $(e_g^2\ t_{2g}^6)$ to $(d_{xy}^2\ d_{z^2}^2, d_{xz}^2, d_{yz}^2)$ causes an increase in the bond strength and additional stabilizing energy to the extent of about $2/3\ \Delta_0$.[26] This contribution must be somewhat diminished by the pairing energy in going from a $(d_{z^2}^1, d_{z^2-y^2}^1)$ to a $(d_{z^2}^2, d_{x^2-y^2}^0)$. This stabilizing energy may cause an enthalpy change favoring the formation of $NiH_{-2}L^{-}$ from $NiH_{-1}L$. Therefore, the value of pK_{1b} becomes smaller than pK_{1a} and the amount of $NiH_{-1}L$ formed is many times less than the amount predicted on purely statistical grounds.

Ni(II)-Tetraglycine

In the case of the Ni(II)-tetraglycine system, all attempts aimed at detecting the intermediate $NiH_{-1}L$ by potentiometry failed and the computer calculation did not converge indicating that its concentration must indeed be almost negligible. However, in Figure 8, the calculations indicate that the more highly deprotonated species $NiH_{-2}L^{-}$ and $NiH_{-3}L^{2-}$ make substantial contributions.

In Figure 11, the experimental points are given as open circles and the best fit is obtained by assuming the deprotonation scheme to be

$$NiL^{+} \rightleftharpoons \underset{\text{(undetectable)}}{(NiH_{-1}L)} \rightleftharpoons NiH_{-2}L^{-} \rightleftharpoons NiH_{-3}L^{2-}$$

which is the result also of the present potentiometric studies. Thus, the sum of the degree of formation of the paramagnetic species is $\alpha_{M^{2+}} + \alpha_{MHL^{2+}} + \alpha_{ML^{+}} + \alpha_{ML_2}$, which implies that both $NiH_{-2}L^{-}$ and $NiH_{-3}L^{2-}$ are diamagnetic. Curve a is the result of this calculation. Curve b assumes that the deprotonation scheme is a one step process as given by Eq. 12. The poorest fit (Curve c) is obtained by assuming that $NiH_{-2}L^{-}$ is present as a paramagnetic species. Therefore, $NiH_{-2}L^{-}$ and $NiH_{-3}L^{2-}$ are concluded to be diamagnetic species. As before, the small deviation of Curve a from the experimental curve in the region from $m = 1$ to $m = 2$ may also be attributed to the presence of a trace amount of nickel(II) hydroxide. The deprotonation from $NiH_{-1}L$ to $NiH_{-2}L^{-}$ involves the structural change from octahedral to square planar, while those involving conversion of NiL^{+} to $NiH_{-1}L$, and $NiH_{-2}L^{-}$ to $NiH_{-3}L^{2-}$, do not. Therefore, on the basis of the reasoning given for the nickel(II)-triglycine system, it is reasonable that the presence of $NiH_{-2}L^{-}$ was detected while that of $NiH_{-1}L$ could not be detected.

The deprotonation from NiL^{+} to $NiH_{-1}L$ for the dipeptide system does not involve a structural change, therefore the stabilizing rearrangement from the octahedral to the square planar configuration is not possible in this system. The titration of the 1:1 nickel(II)-dipeptide system was not measured above $m = 1.2$ because of the formation of precipitate. This difficulty was overcome by the use of a new ligand, the Schiffs base of a dipeptide with a ketone, such as 2-pyridyl methyl ketone. This Schiff base forms the intermediate complex NiL^{+}, which readily dissociates one peptide proton to form the more stable diamagnetic square planar complex $NiH_{-1}L$

This diamagnetic complex $NiH_{-1}L$ for the 1:1:1 nickel(II):2-pyridylmethylketone:glycyl-DL-alanine system was found to have a very high molar extinction coefficient. ($\epsilon_{max} = 3.19 \times 10^3$; $\lambda_{max} = 380$ nm). The proton dissociation constant for conversion of the chelate NiL^{+} to $NiH_{-1}L$ was found to have the value $-\log K_{1a} = 7.24 \pm 0.03$ from a study of absorption spectra, which is even lower than that

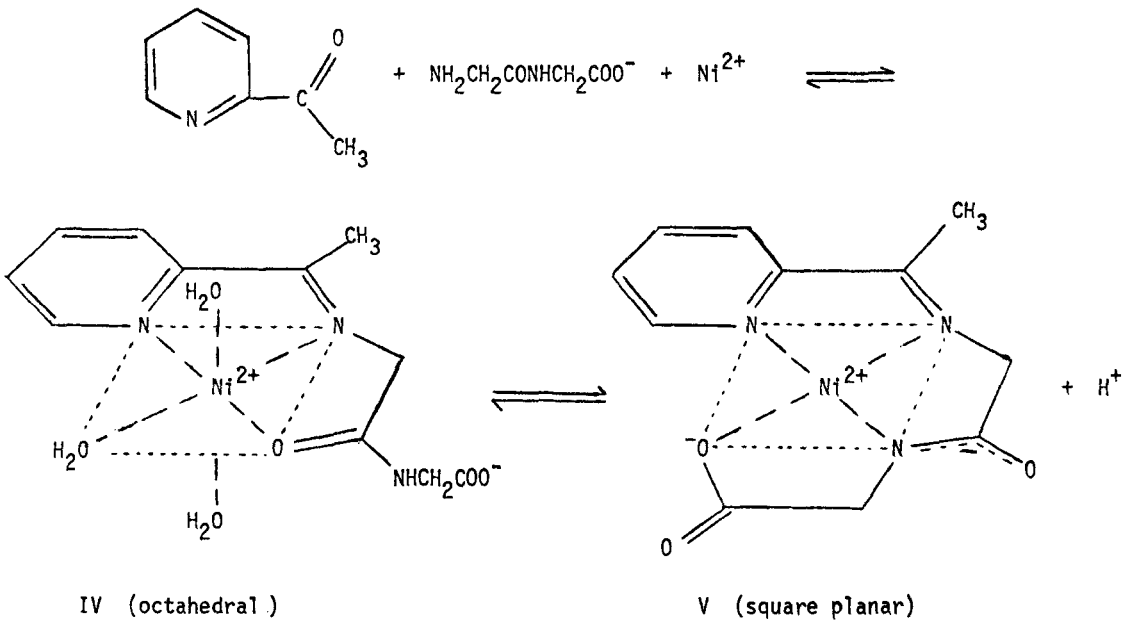

IV (octahedral) V (square planar)

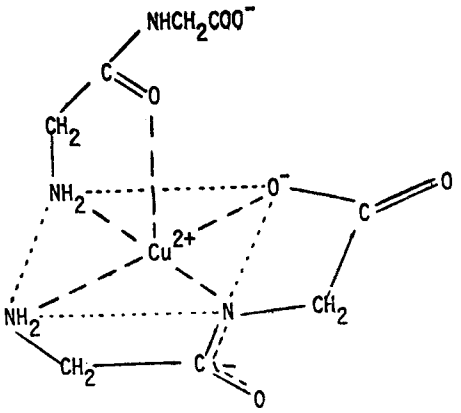

VI $Cu(H_{-1}L)L^-$ (gg)

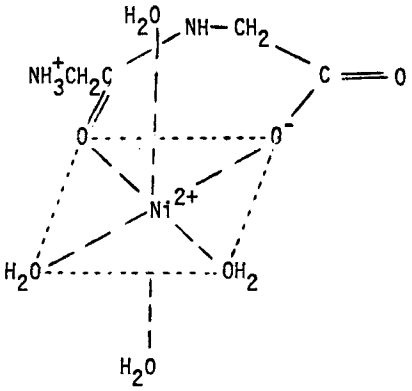

IX $NiHL^{2+}$ (gg) (octahedral)

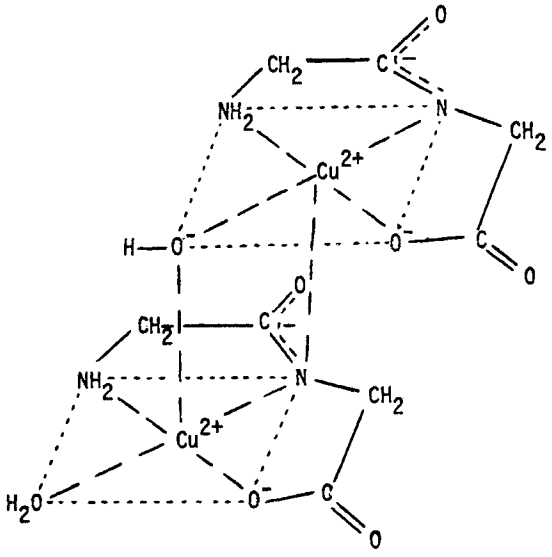

VII $(CuH_{-1}L)_2OH^-$ (gg)

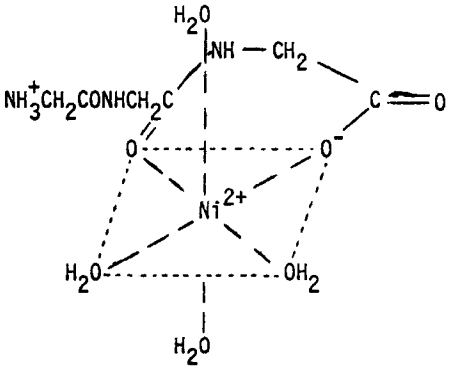

X $NiHL^{2+}$ (ggg) (octahedral)

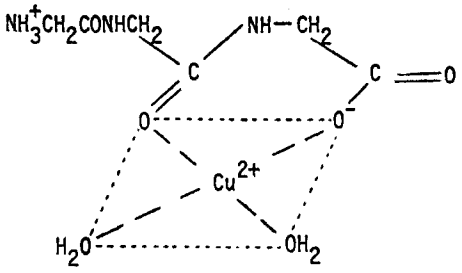

VIII $CuHL^{2+}$ (ggg)

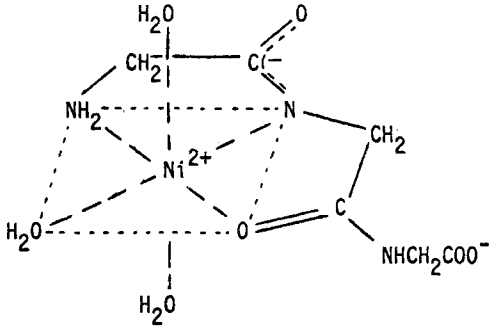

XI $NiH_{-1}L$ (ggg) (octahedral)

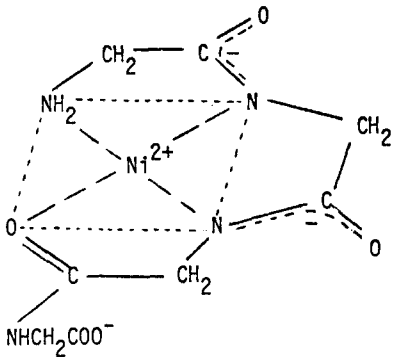

XII $NiH_{-2}L^-$ (gggg) (square planar)

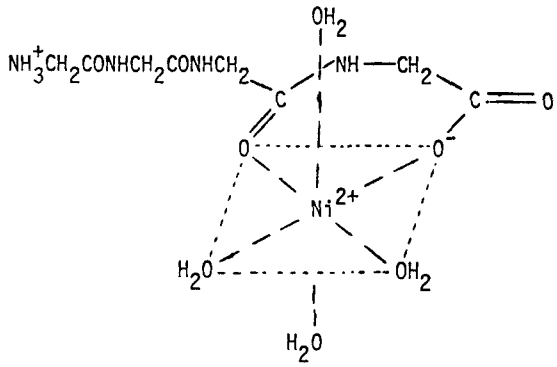

XIII $NiHL^{2+}$ (gggg)

of the nickel(II)-triglycine system $-\log K_{1b} = 7.85$ (conversion $NiH_{-1}L$ to $NiH_{-2}L^-$). It may, therefore, be inferred that at least two potentially trigonal nitrogens are necessary to form stable square planar nickel(II) complexes in systems of this type.

Structures of Chelates

The earlier suggestions for the bonding modes of the low pH Cu(II)-polyglycine and nickel(II)-polyglycine complexes[1,2,3] in which peptide protons are not displaced, were later revised by Martell[7,8] after a detailed study of Kim's IR data.[5] It is now generally agreed that the structures of these complexes in solution, having the general formula ML^+, involve a five membered chelate ring in which the metal ion coordinates to the terminal amino group and the adjacent peptide carbonyl oxygen. The peptide carbonyl IR band at 1670 cm^{-1}, in the case of the copper(II)-diglycine complex, for example, shifts to lower frequency, 1625 cm^{-1}, by 45 cm^{-1}, when it becomes coordinated to the copper(II) ion. Structural considerations, reinforced by a study of molecular models, indicates that coordination of the N-terminal amino group and the adjacent carbonyl oxygen atom to the metal ion requires that the rest of the ligand remain uncoordinated, as shown in formulas II, III and VI. These structures are in good agreement with the structure found in solid state.[6]

As the basicity of the solution increases, the +I effect of the central metal ion results in the displacement of the peptide proton to form the negative amino nitrogen, which has greater coordination affinity for the metal ion than does the carbonyl oxygen. Additional stabilization may be attributed to the fact that the formation of the $MH_{-1}L$ species results in the formation of two five membered rings. Thus the number of chelate rings increases in going from ML^+ to $MH_{-n}L^{(n-1)-}$.

The electronic spectra of the copper(II)-triglycine system in Figure 9 show that the most significant absorption band shifts to lower wavelength as base is added. This change in the ligand field spectra indicates an increase in the number of chelate rings and/or a substantial increase in the number of coordinate covalent bonds involving the metal ion.

The results discussed above indicate that meaningful interpretations of microscopic data such as IR, nmr, esr and electronic spectra of ionic species in aqueous solution should be based on the adequate knowledge of the ionic species distribution in solution, which is provided mainly by careful potentiometric studies of the metal complex systems involved. Formulas I-III and VI-XIII indicate the solution structures and coordinate bonding modes that are believed to be evident on the basis of the present potentiometric, spectrophotometric and magnetic data. These structures have not been proposed elsewhere. Additional suggestions for the structures of remaining complex species that appear in the distribution curves (Figures 1–8), but not illustrated in this paper, have been provided by Martell and Kim.[8]

REFERENCES

1. M. K. Kim and A. E. Martell, *Biochem.*, **3**, 1169 (1964).
2. M. K. Kim and A. E. Martell, *J. Amer. Chem. Soc.*, **88**, 914 (1966).
3. M. K. Kim and A. E. Martell, *ibid*, **89**, 5138 (1967).
4. M. K. Kim and A. E. Martell, *ibid*, **85**, 3080 (1963).
5. M. K. Kim, Ph.D. Thesis, Illinois Institute of Technology, June, 1966.

6. H. C. Freeman in *The Biochemistry of Copper*, J. Peisach, P. A. Isen, and W. E. Blumberg, Ed., Academic Press, Inc., New York, N.Y., 1966, p. 77.
7. A. E. Martell in *Recent Topics in Coordination Chemistry*, S. Misumi and K. Ueno Eds., Special Publication No. 84, Nankodo Publishing Co., 1968, p. 47.
8. A. E. Martell and M. Kim, *Coordination Chemistry*. In press.
9. R. Osterberg and B. Sjioberg, *J. Biol. Chem.*, **243**, 3038 (1968).
10. M. K. Kim and A. E. Martell, *J. Amer. Chem. Soc.*, **91**, 872 (1969).
11. R. B. Martin, M. Chamberlin and J. T. Edsall, *ibid.*, **82**, 495 (1960).
12. A. P. Brunetti, M. C. Lim and G. H. Nancollas, *ibid*, **90**, 5120 (1968).
13. R. P. Martin, *Bull. Soc. Chim. France*, **63**, 1136 (1967).
14. W. L. Koltun and F. R. N. Gurd, *J. Biol. Chem.*, **238**, 124 (1963).
15. J. L. Biester and P. M. Ruoff, *J. Amer. Chem. Soc.*, **81**, 6517 (1959).
16. H. Dobbie and W. O. Kermack, *Biochem. J.*, **59**, 246 (1955).
17. A. M. Bond, *Coord. Chem. Rev.*, **6**, 377 (1971).
18. F. J. C. Rossotti and H. Rossotti, *J. Chem. Ed.*, **42**, 375 (1965).
19. H. S. Harned and B. B. Owen, *The Physical Chemistry of Electrolytic Solutions*, 2nd Ed., Reinhold Publishing Corp., New York, N.Y., 1958, p. 483, 523, 578.
20. D. F. Evans, *J. Chem. Soc.*, 2003 (1959).
21. G. Schwarzenbach, A. Willi, and R. O. Bach, *Helv. Chim. Acta*, **30**, 1303 (1947).
22. L. G. Sillen, *Acta Chem. Scand.*, **16**, 159 (1962).
23. N. Ingri and L. G. Sillen, *Acta Chem. Scand.*, **16**, 173 (1962).
24. A Kaneda and A. E. Martell, unpublished results; A. Kaneda, Ph. D. Dissertation, Texas A & M University, January, 1973.
25. E. J. Billo and D. W. Margerum, *J. Amer. Chem. Soc.*, **92**, 6811 (1970).
26. F. A. Cotton and G. Wilkinson in *Advanced Inorganic Chemistry*, Interscience Publishers, New York, 2nd. Ed., 1967, p. 713.